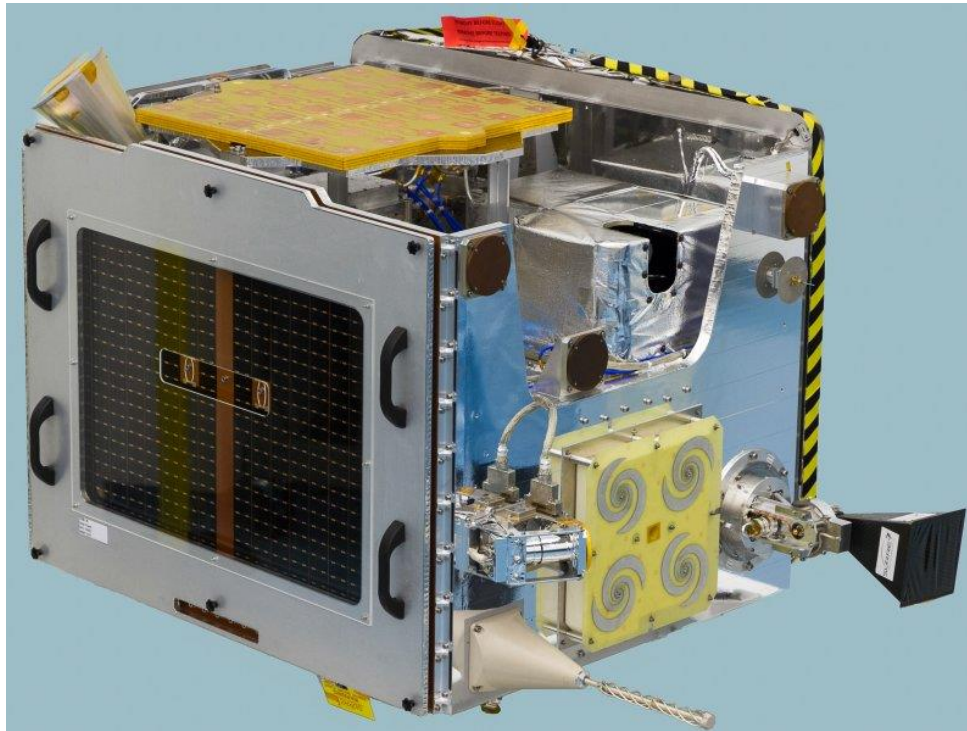


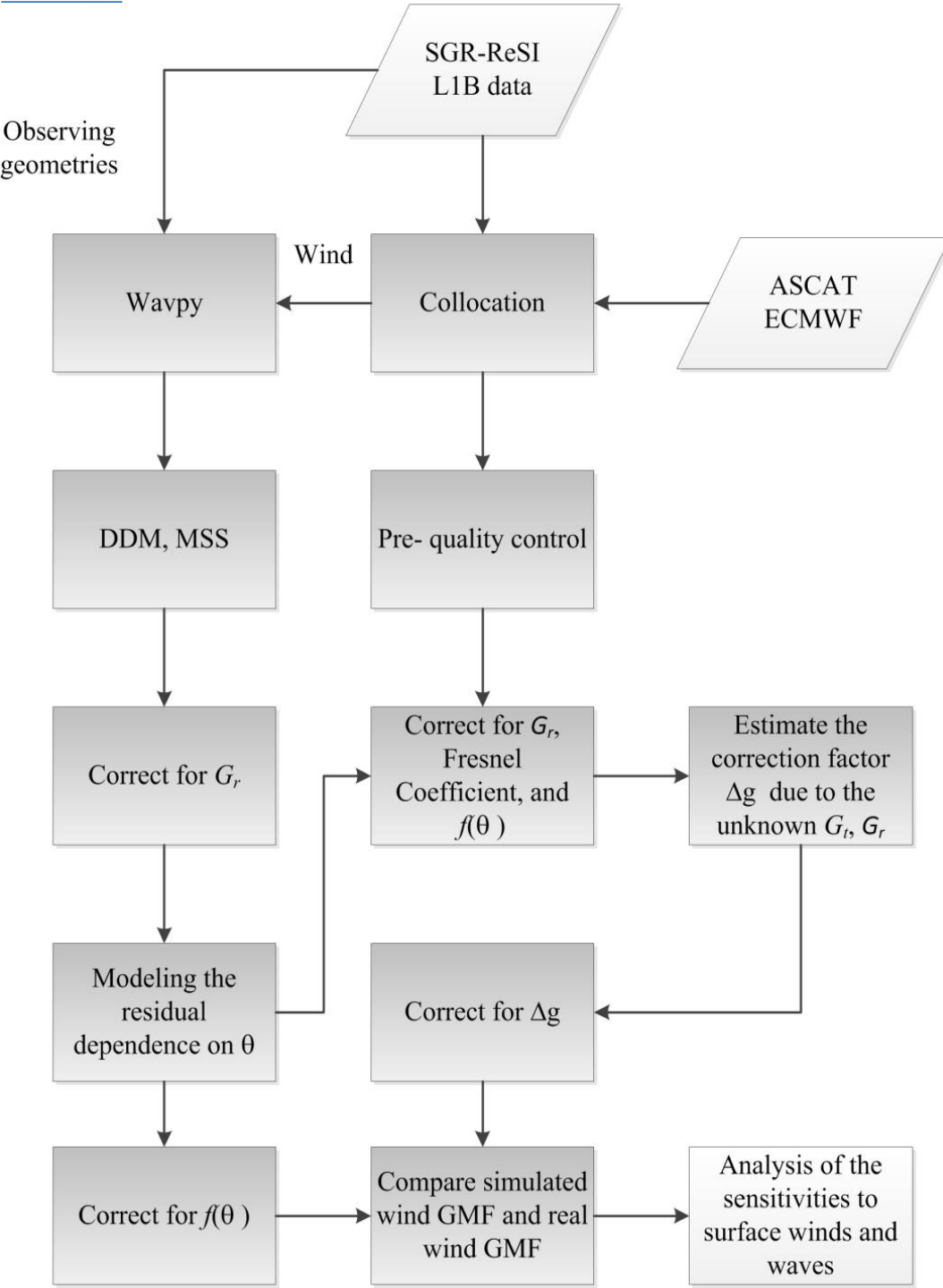
GMF development for GNSS-R

Wenming Lin, Marcos Portabella



$$\left\langle \left| Y(\Delta\tau, \Delta f) \right|^2 \right\rangle = \frac{p_t}{(4\pi)^3} \lambda^2 T_c^2 \int d\vec{\rho} \frac{G_T(\vec{\rho}) G_R(\vec{\rho}) \sigma^0(\vec{\rho}) \Lambda^2(\tau + \Delta\tau(\vec{\rho})) \left| S(\delta f(\vec{\rho})) \right|^2}{R_{T,\rho}^2 R_{R,\rho}^2}$$

1. Definition of observable
2. Data
3. SNR corrections with simulated data
4. SNR corrections with real data
5. Analysis
 - Observable vs ECMWF wind speed
 - Observable vs ASCAT wind speed
 - Observable vs wave parameters
6. Wind validation: Triple collocation ASCAT-TDS-ECMWF
7. Conclusions

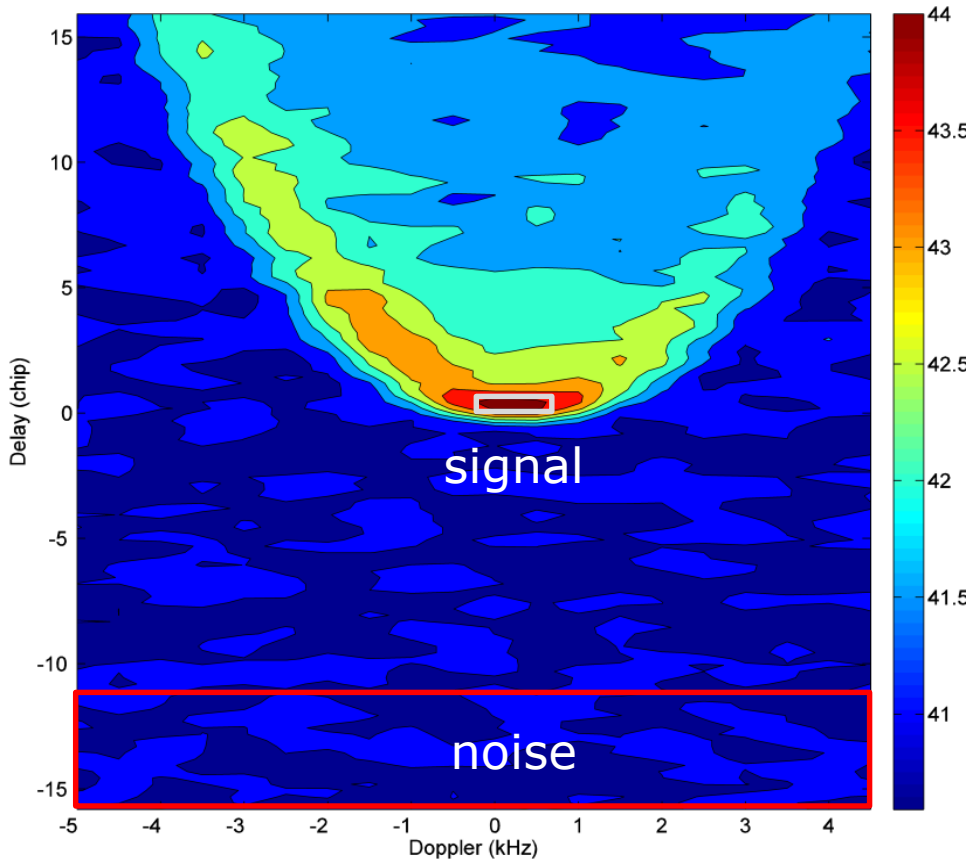


Pre-QC rejection (any of below criteria):

- $\text{Peak}/\text{SD}_{\text{noise}} < 4$;
- $x_{\text{peak}} - x_{\text{SP}} \notin [0, 4]$;
- $|\text{latitude}| > 80^\circ$;
- $G_r < 0$ dB;
- $\text{SST} < 1^\circ \text{C}$;
- InEclipse;
- DirectSignalInDDM;
- DDMPixelNoiseInvalid;
- LandFlag;

Fig.1 Study flow

1. Definition of observable



Signal: the average of the peak power across certain Doppler and delay bins (3 Doppler bins \times 1 delay bin, as indicated by the gray rectangle) subtracted by the noise.

Noise: the average of the noise floor across all Doppler bins and the first 20 negative delay bins of the DDM

Fig. 2 Illustration of the observable definition

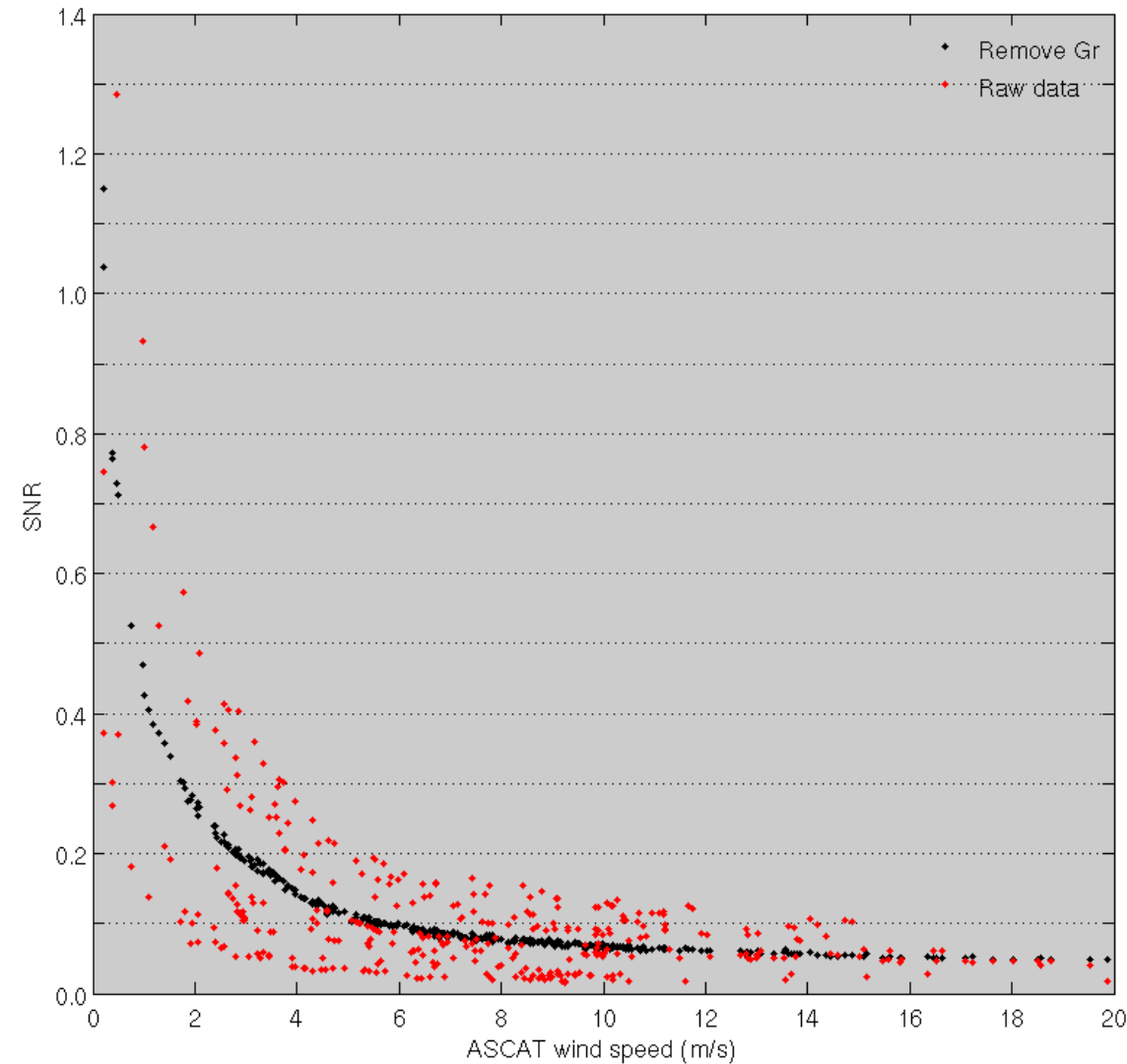
$$SNR = \frac{signal - noise}{noise}$$

2. Data

Table 1 List of the collocated ancillary parameters

Parameters		Source
Wind speed and direction	<input checked="" type="radio"/>	ECMWF/ASCAT
Significant wave height (H_s)	<input checked="" type="radio"/>	ECMWF
Sea surface temperature (SST)	<input checked="" type="radio"/>	ECMWF
Air density		ECMWF
Mean wave direction		ECMWF
Peak period of 1D wave spectra		ECMWF
Mean wave period		ECMWF
Mean square slope	<input checked="" type="radio"/>	ECMWF
Surface wind variability indicator	<input checked="" type="radio"/>	ASCAT

3. SNR corrections with simulated data



The primary issue of GMF development is to correct for the effect of **receiver antenna gain**.

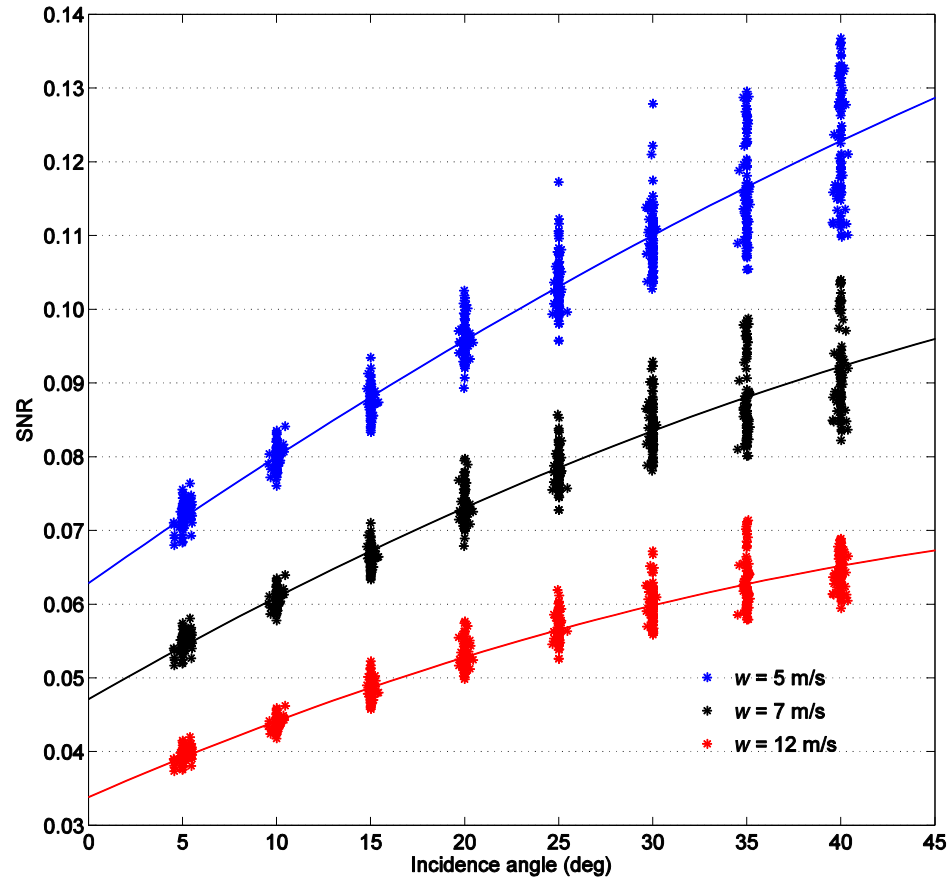
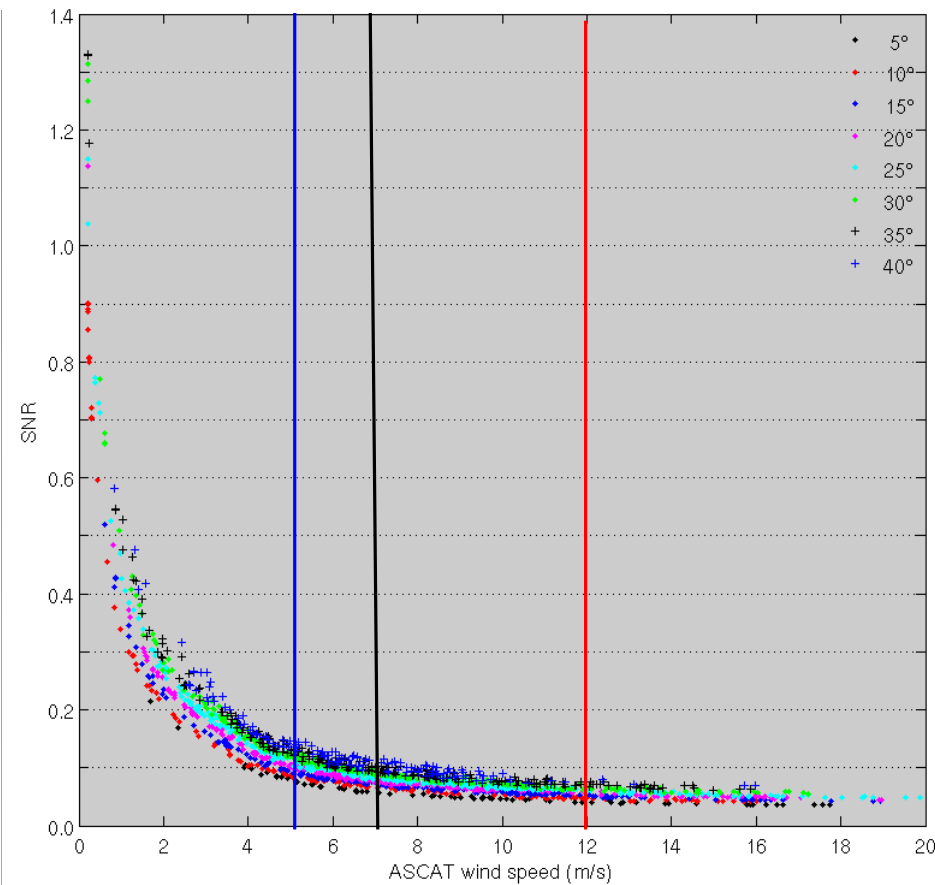
$$SNR_1 = \frac{SNR_0}{G_r}$$

Red dots: raw SNR (wavpy)

Black dots: after decoupling the effect of receiver antenna gain G_r

Incidence angle $\theta = 25^\circ \pm 0.5^\circ$

3. SNR corrections with simulated data

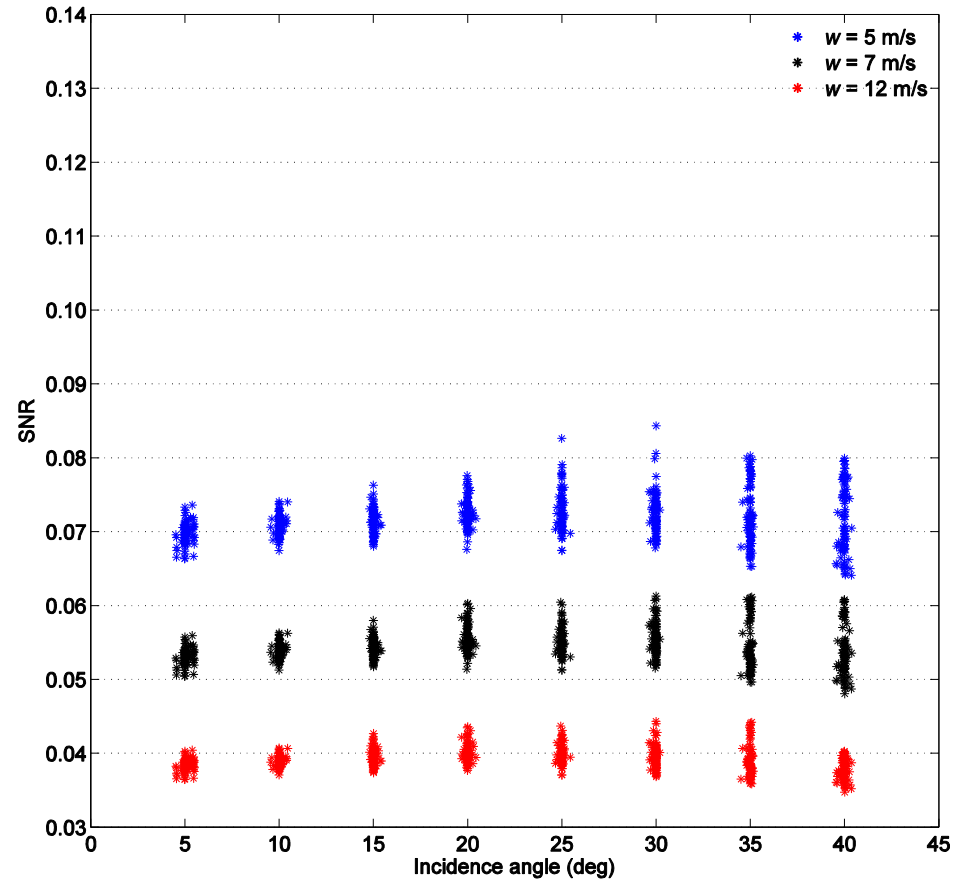
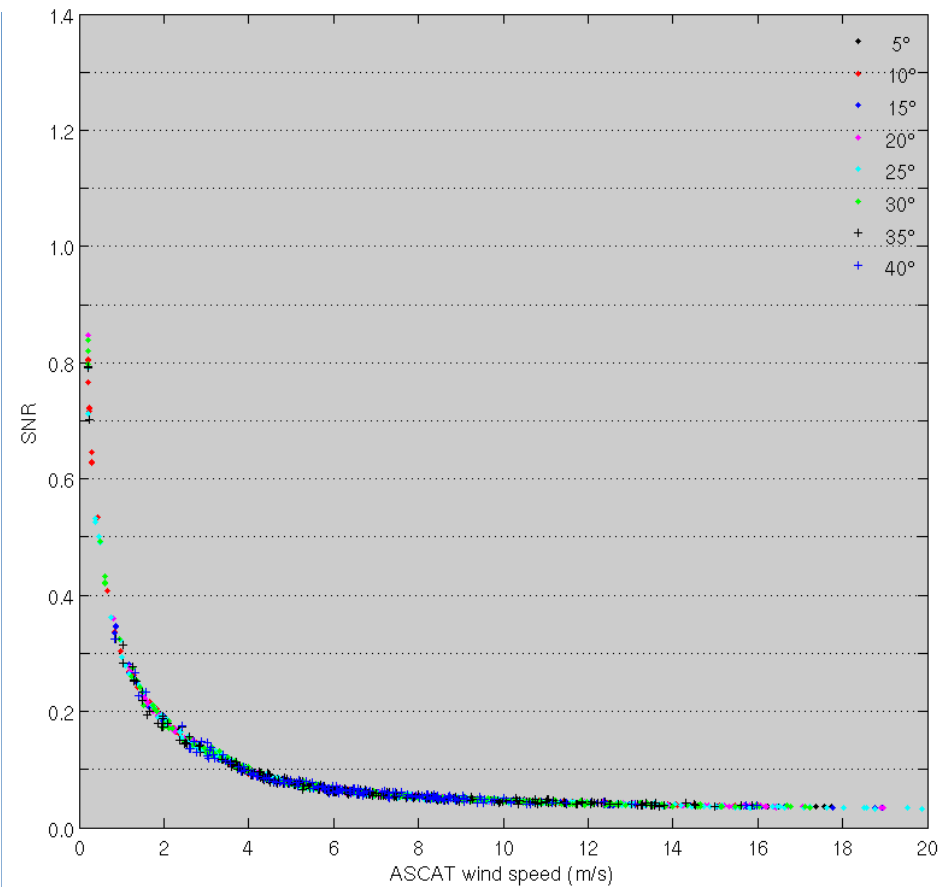


After correcting for the receiver antenna gain G_r , SGR-ReSI SNR as a function of wind speed (left) and incidence angle (right)

The residual dependence on incidence angle is attributed to:

- surface area (corresponding to the signal zone);
- transmitter gain;
- distance from specular point to transmitter/receiver.

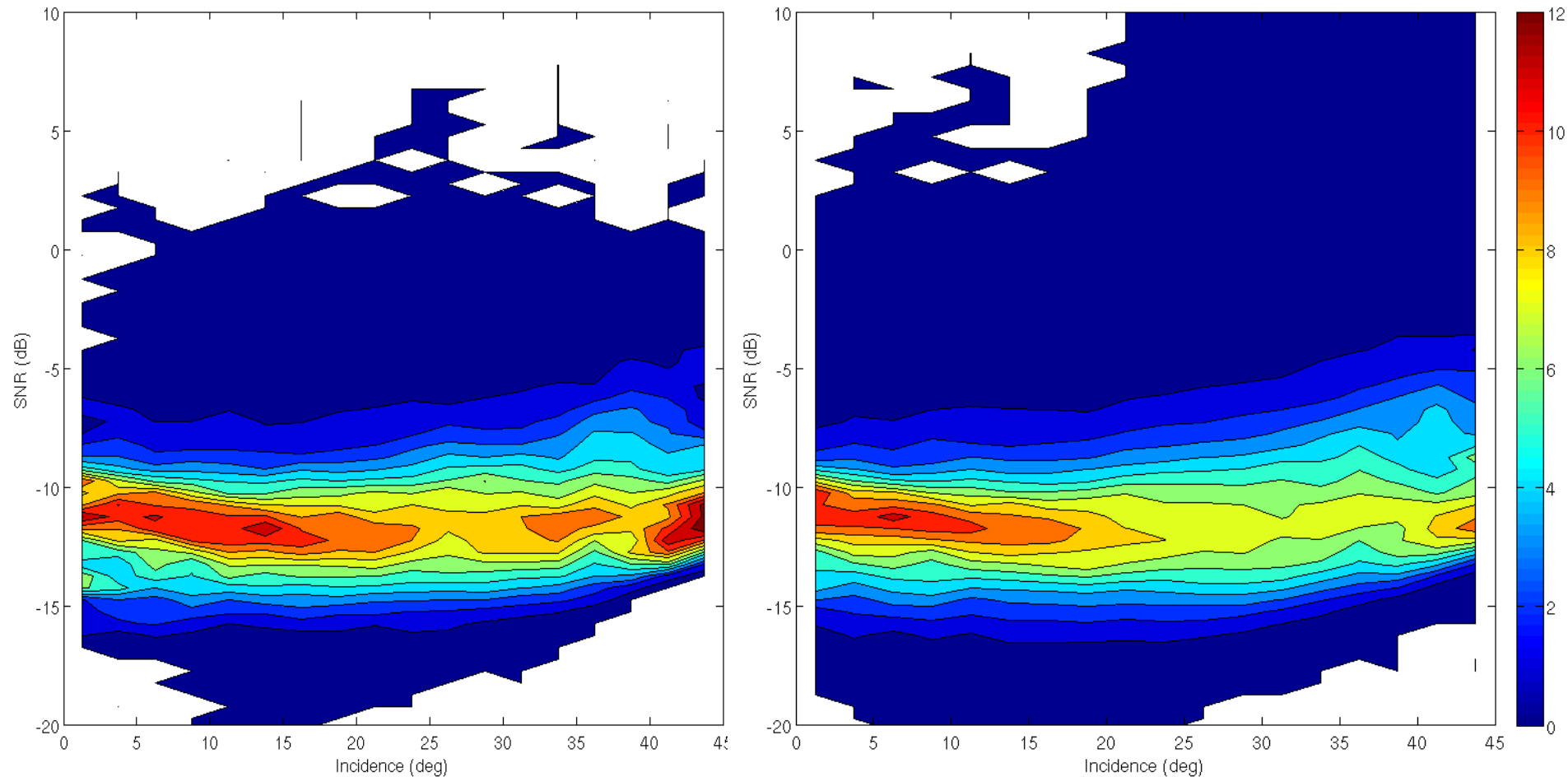
3. SNR corrections with simulated data



$$SNR_2 = \frac{SNR_1}{f(\theta)}$$

$$f(\theta) = 0.019426\theta + 0.93379$$

4. SNR corrections with real data

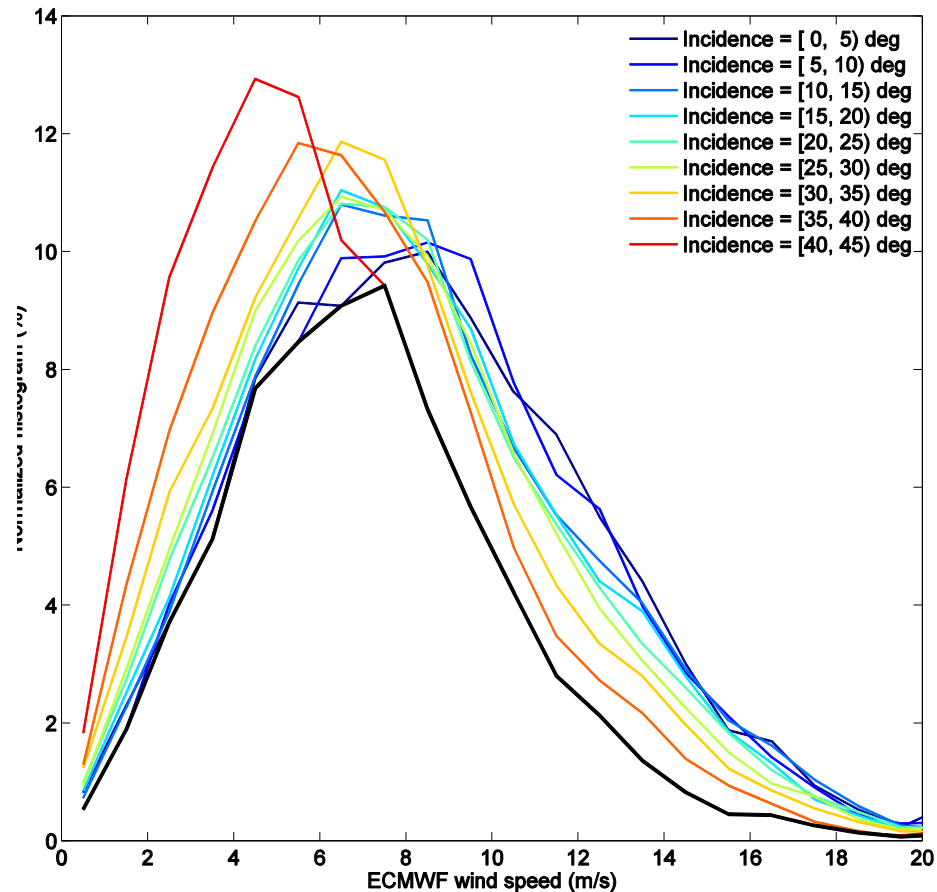
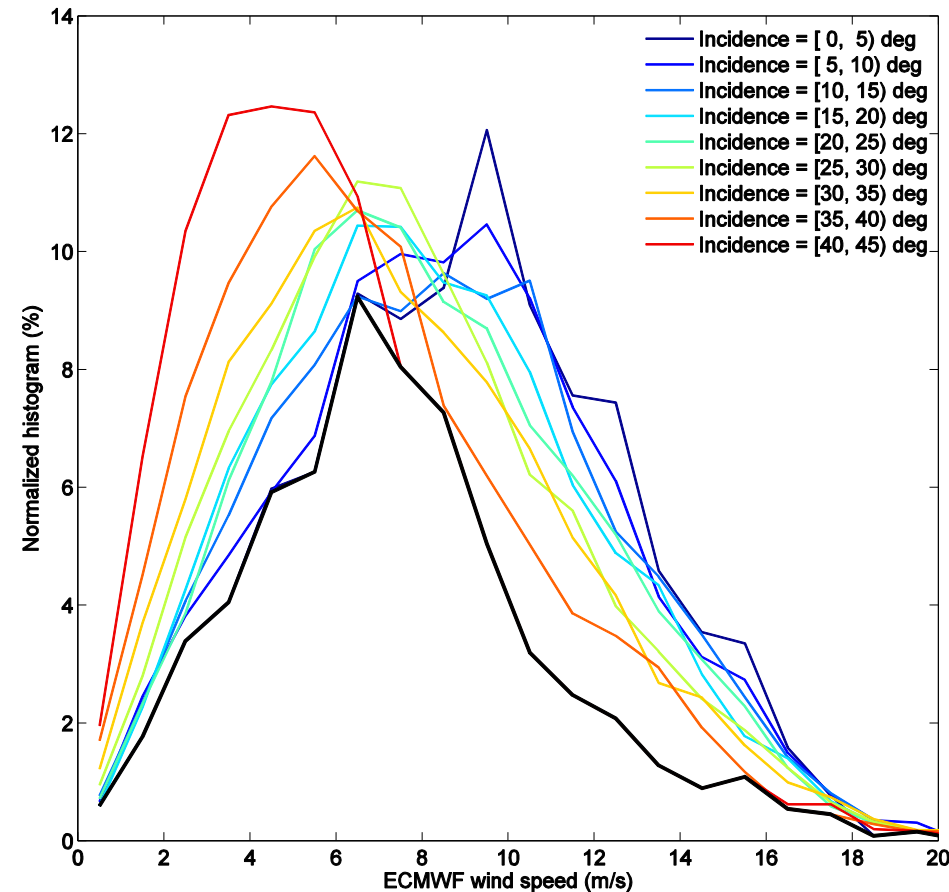


Unmonitored automatic gain control mode (UAGC)

Fixed gain mode (FGC)

2D histogram of SNR_2 versus incidence angle

4. SNR corrections with real data



Unmonitored automatic gain control mode (UAGC)

Fixed gain mode (FGC)

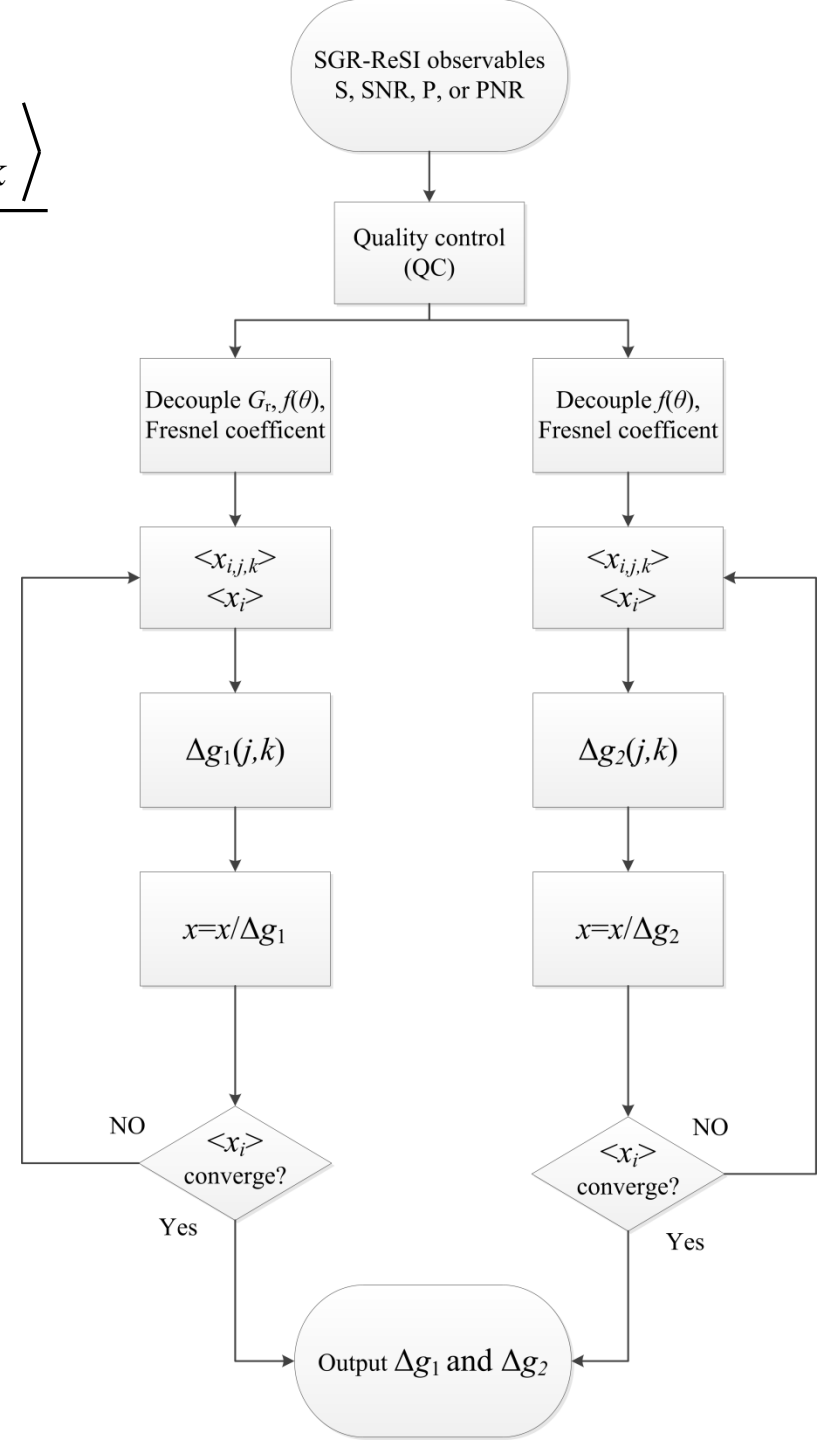
Wind speed histogram for different incidence angles (color)
Black curves indicated the matched PDF for the previous slide

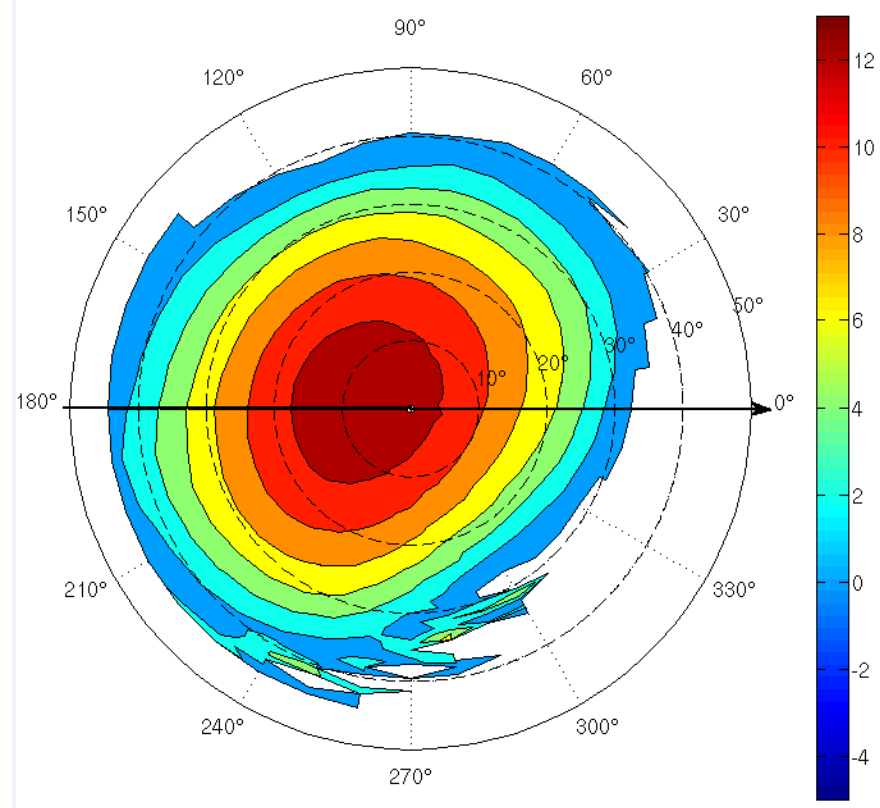
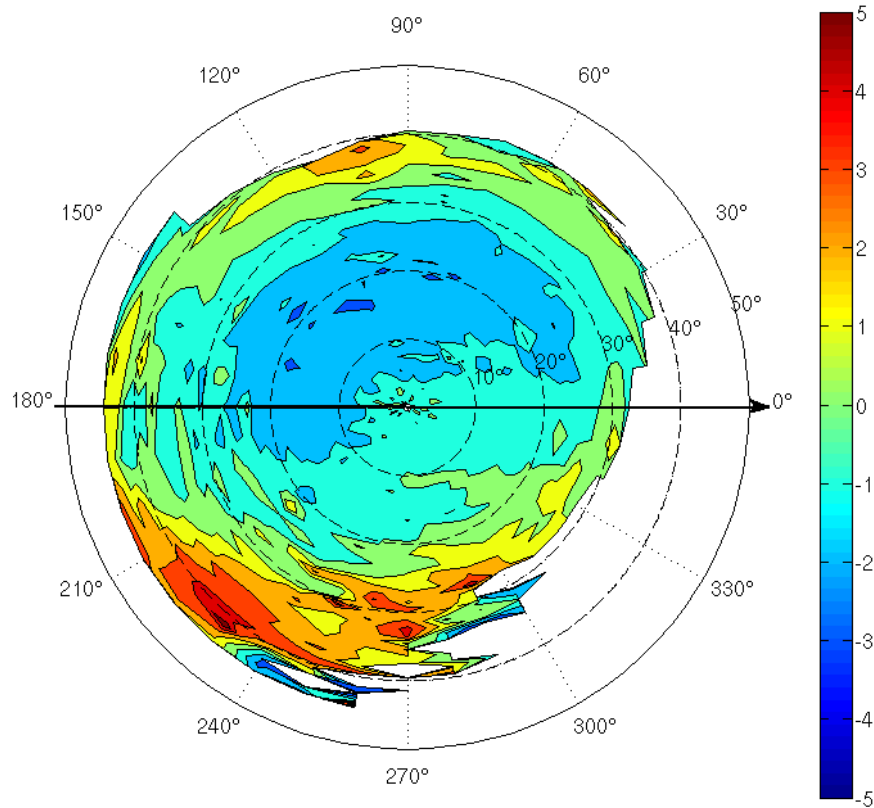
$\Delta g(\theta, \varphi)$ estimation

$$\Delta g_{j,k} = \frac{1}{N} \sum_i \frac{n_i \cdot \langle x_{i,j,k} \rangle}{\langle x_i \rangle}$$

Remarks:

- i, j, k represent the bin number of wind speed, incidence angle, and azimuth angle (SP to Receiver vector in the receiver's antenna frame), respectively.
- bin size: 1 m/s for i , 1° for j , and 10° for k .
- Fresnel coefficient is calculated using the collocated ECMWF SST data ;
- The estimation of Δg generally converges after three iterations.
- Δg_1 consists of the contribution from transmitter antenna gain, and the unknown bias of receiver antenna gain.
- Δg_2 consists of Δg_1 and receiver antenna gain



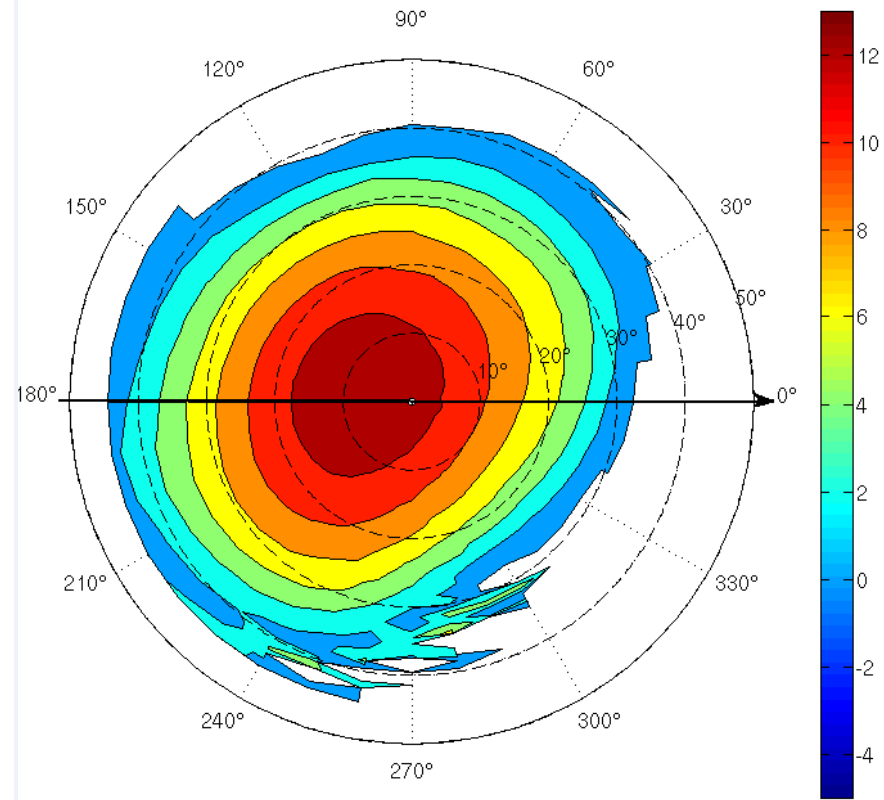
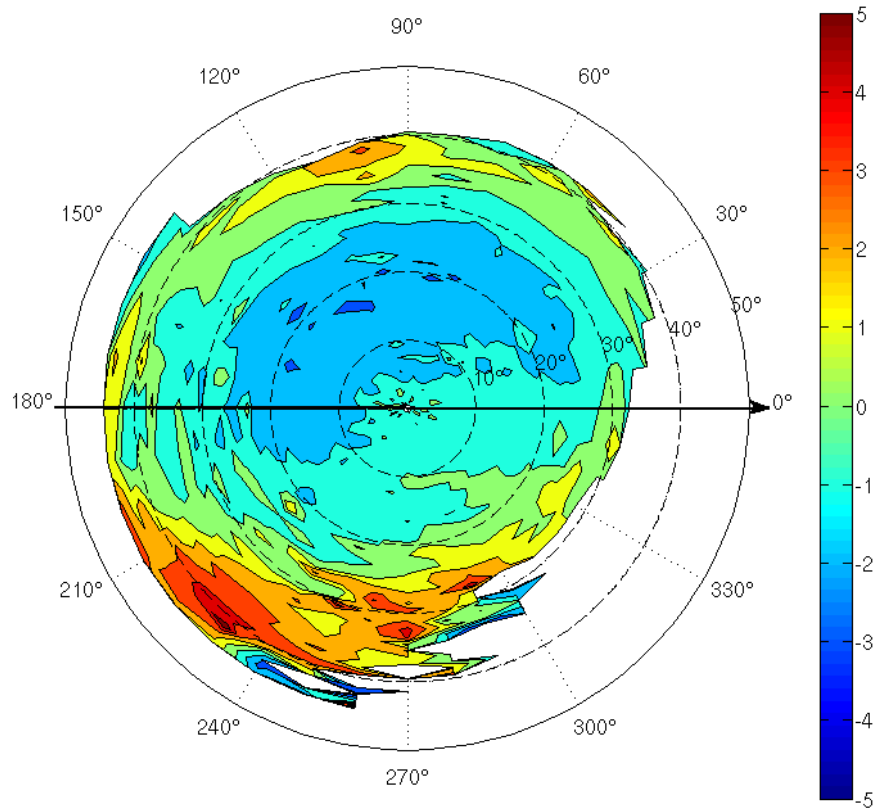


$$\Delta g_1(\theta, \varphi)$$

Further calibration factor
(combined receiver & transmitter G)

$$\Delta g_2 / \Delta g_1$$

Inferred receiver
antenna gain pattern

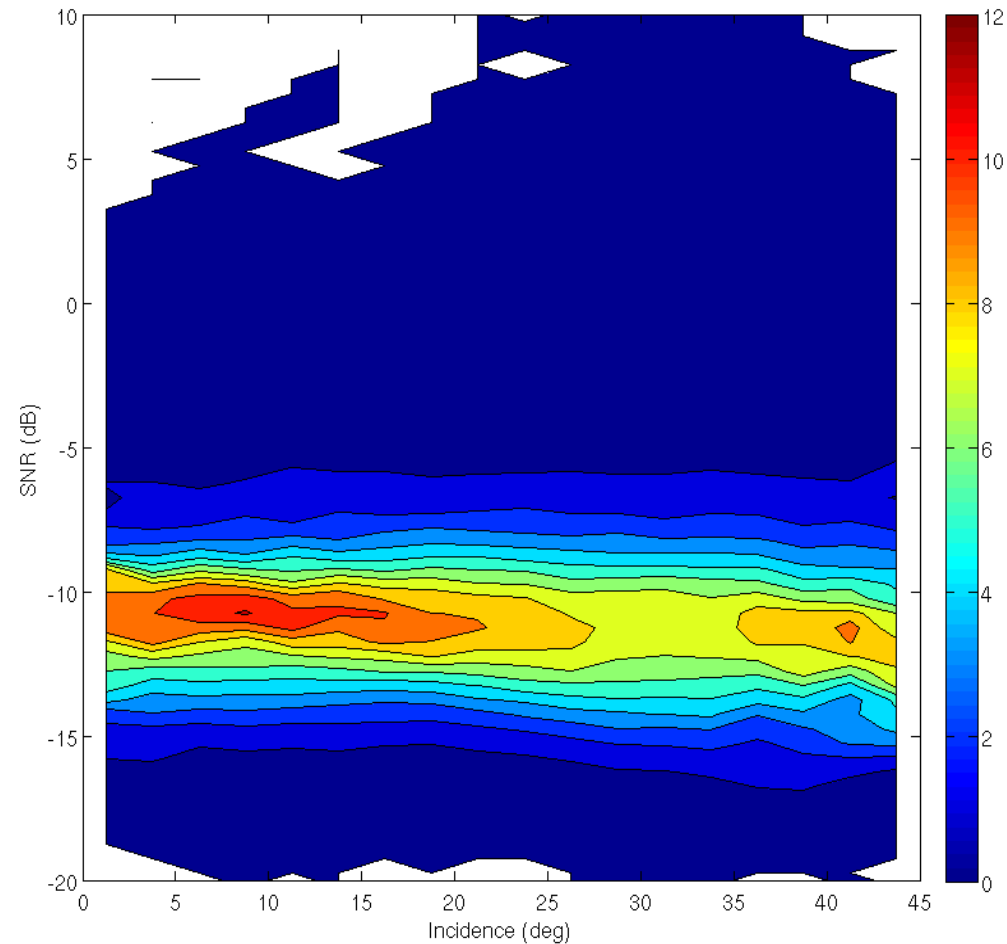
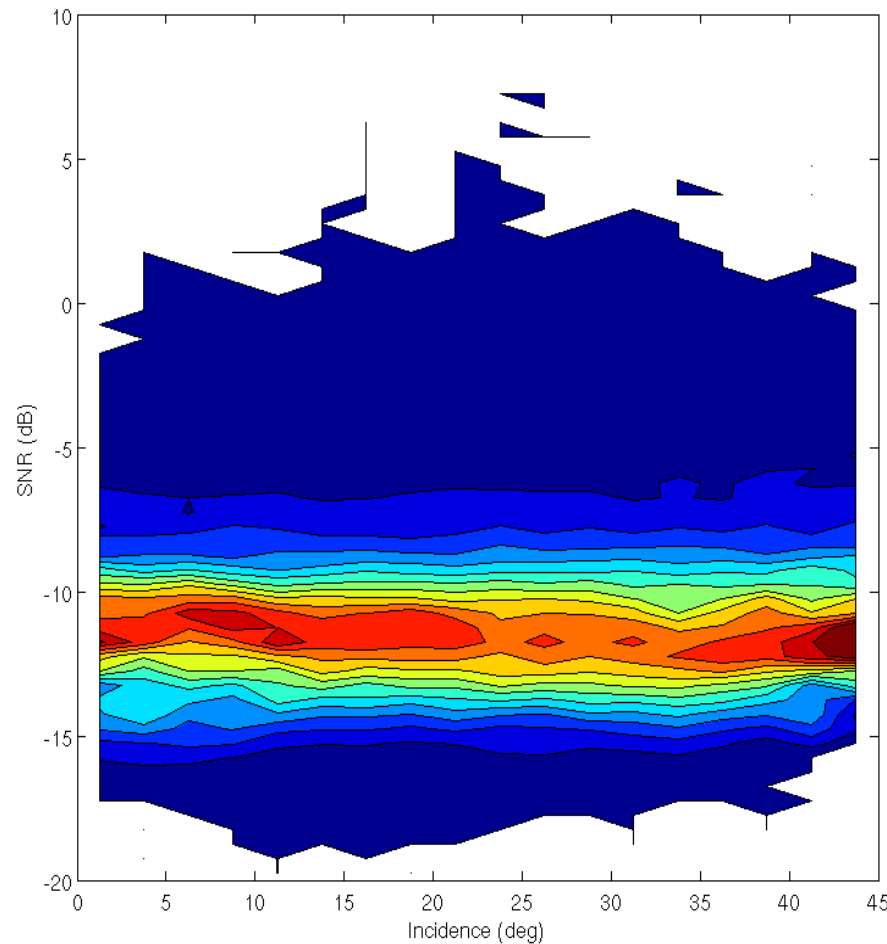


$$\Delta g_1(\theta, \varphi)$$

Further calibration factor
(combined receiver & transmitter G)

Real receiver antenna
gain pattern

4. SNR corrections with real data



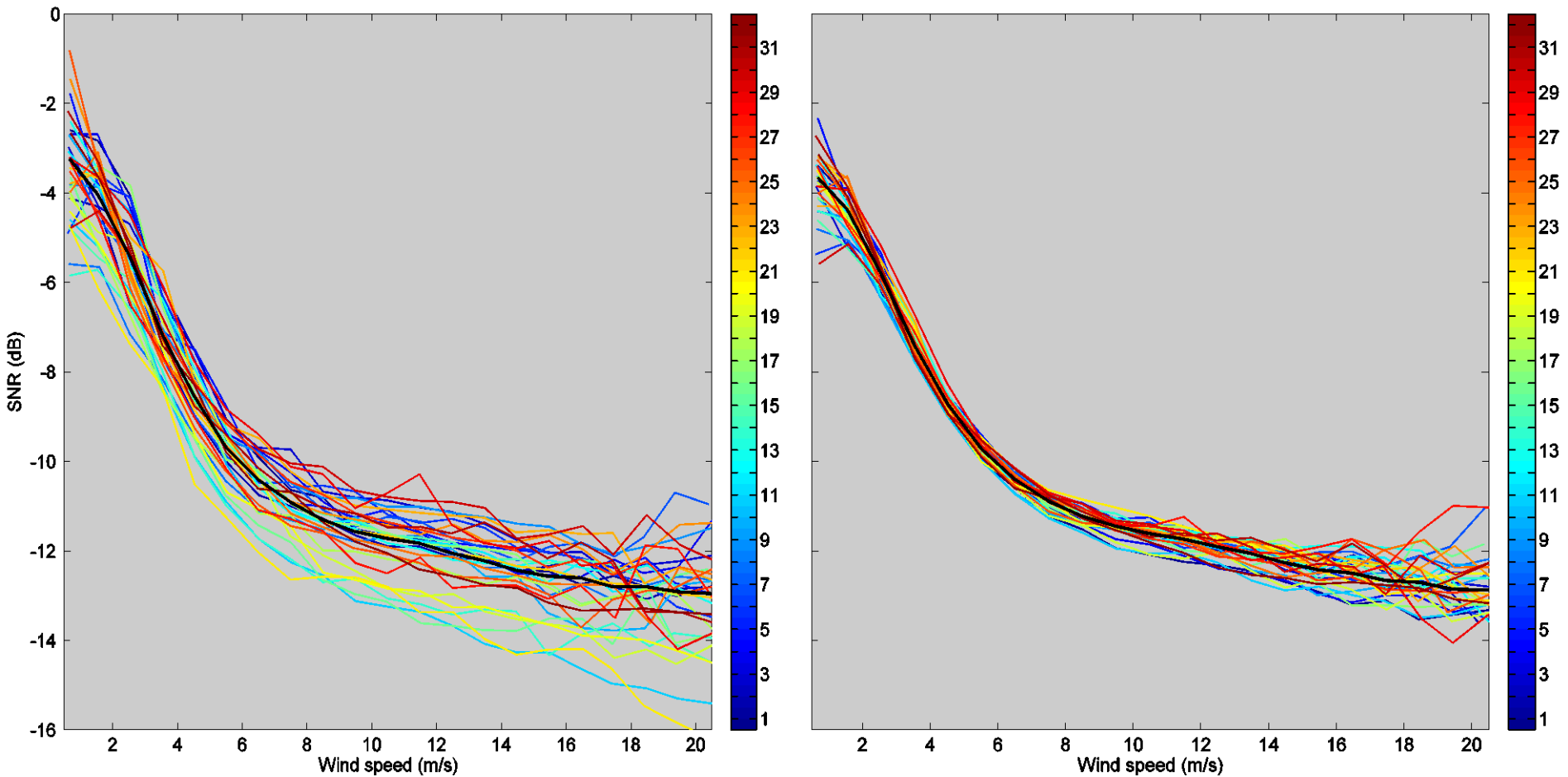
Unmonitored automatic gain control mode (UAGC)

Fixed gain mode (FGC)

2D histogram of SNR_3 versus incidence angle

$$SNR_3 = \frac{SNR_2}{\Delta g_1}$$

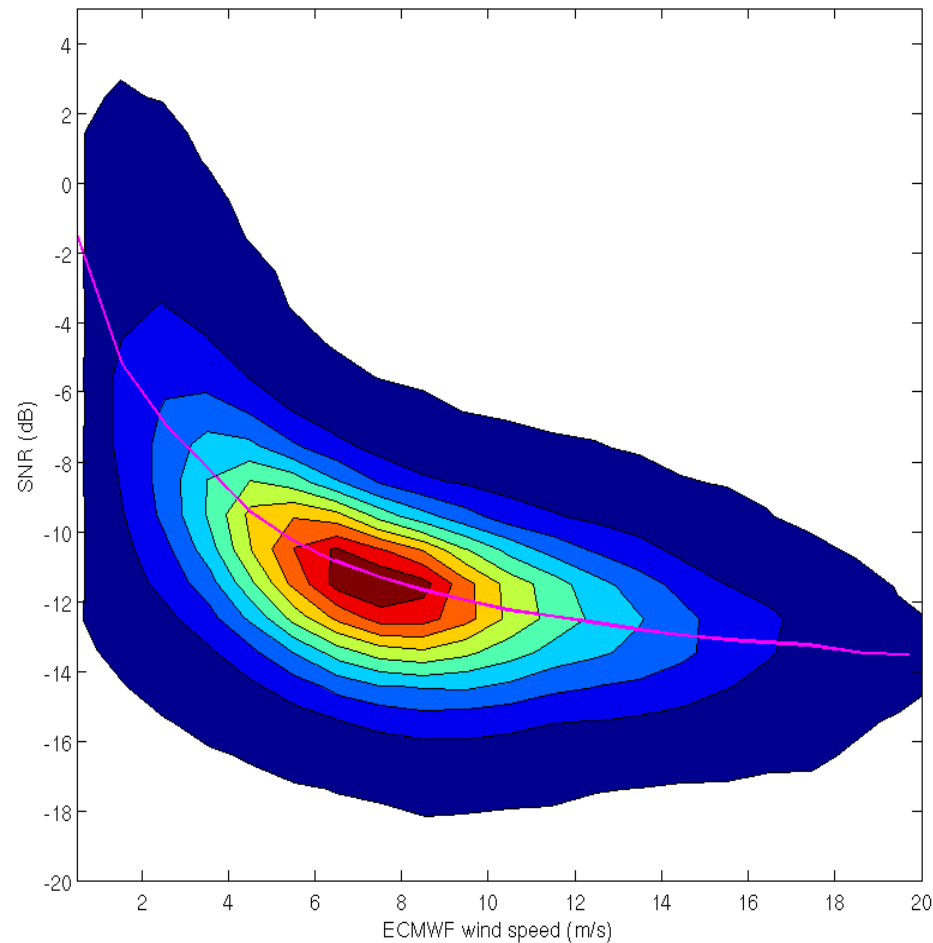
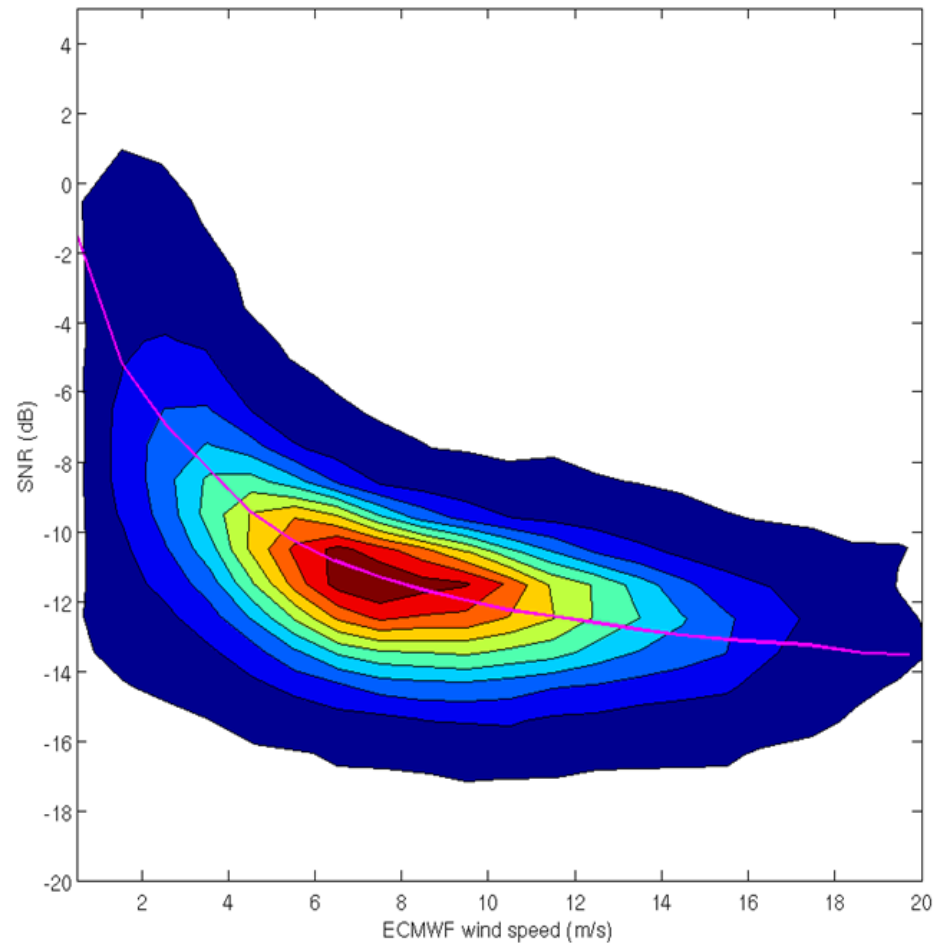
4. SNR corrections with real data



$$SNR_3 = \frac{SNR_2}{\Delta g_1}$$

$$SNR_4 = \frac{SNR_2}{\Delta g_{PRN}}$$

5. Analysis: observable vs ECMWF wind speed

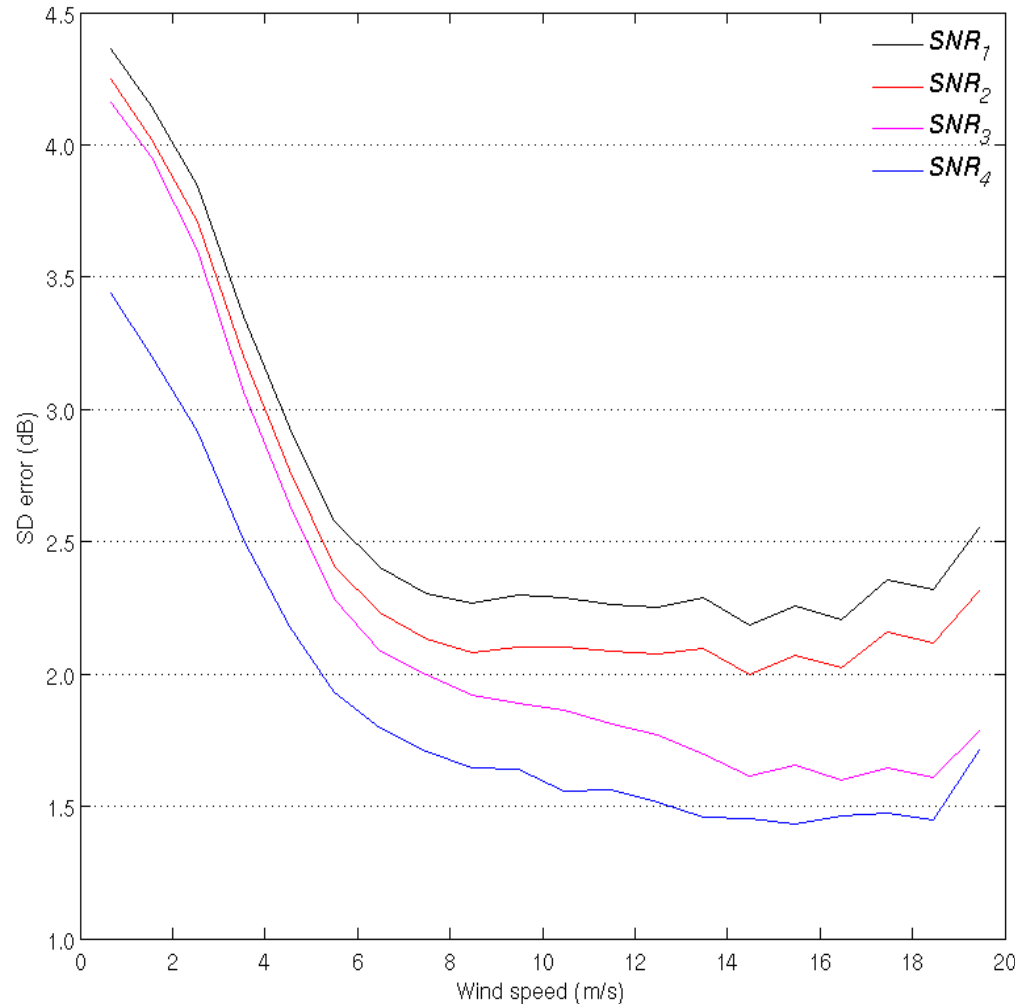


Unmonitored automatic gain control mode (UAGC)

Fixed gain mode (FGC)

Contour plot of SNR_3 versus ECMWF wind speed, for the (a) UAGC mode and the (b) FGC mode. The magenta curve shows the theoretical wind GMF derived from the Wavpy simulation

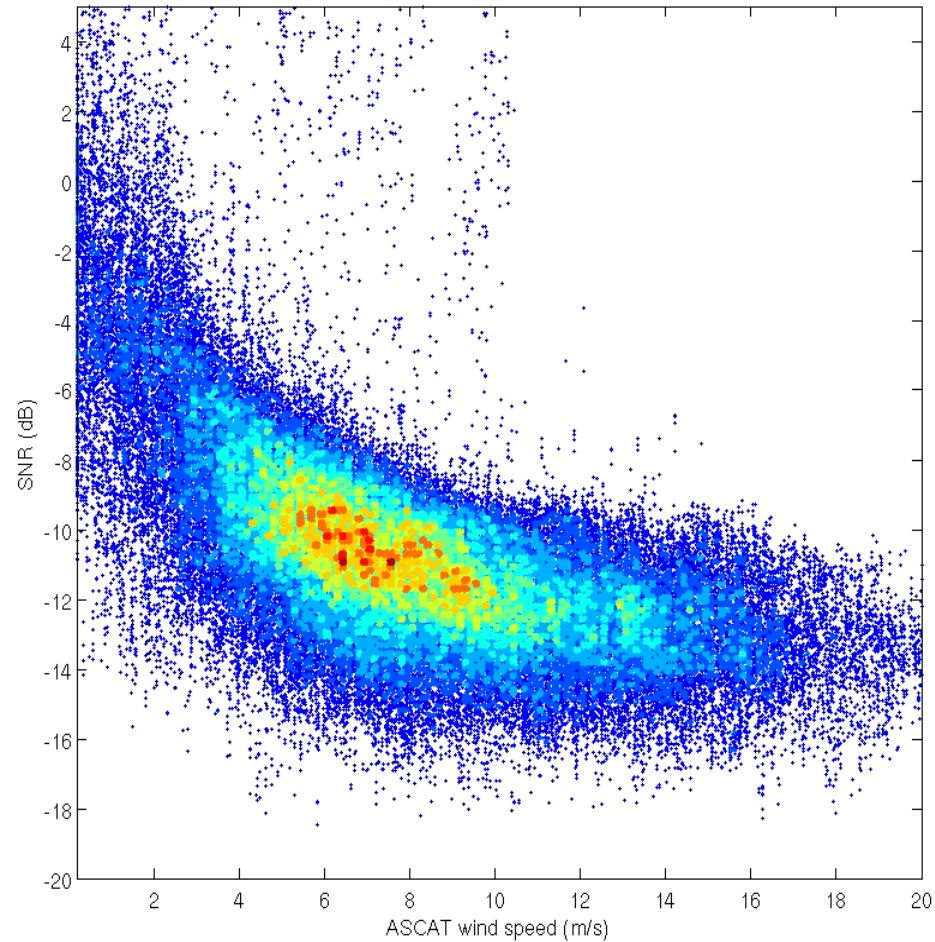
5. Analysis: observable vs ECMWF wind speed



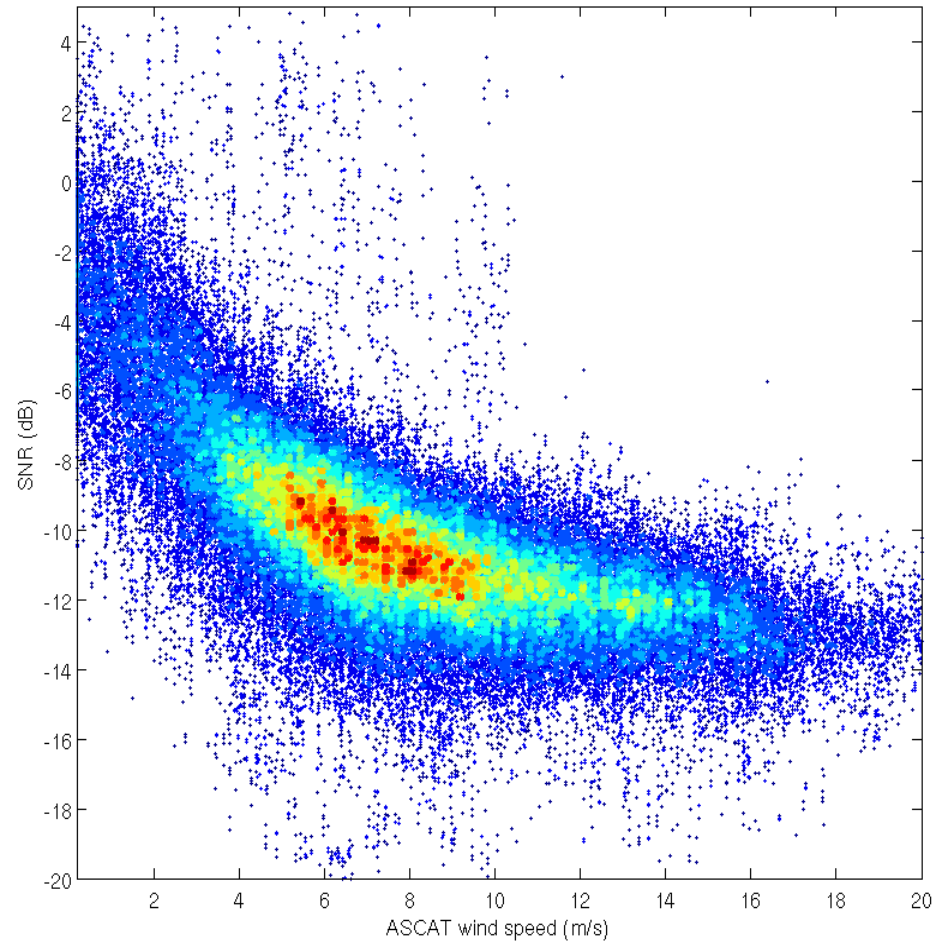
- Subscript '1', observable after correcting for G_r and Fresnel coefficient;
- Subscript '2', observable after correcting for G_r , Fresnel coefficient and $f(\theta)$;
- Subscript '3', observable after correcting for G_r , Fresnel coefficient, $f(\theta)$ and Δg_1 ;
- Subscript '4', observable after correcting for G_r , Fresnel coefficient, $f(\theta)$ and Δg_{PRN} .

FGC mode, the SD errors as a function of wind speed for different $SNRs$

5. Analysis: observable vs ECMWF wind speed

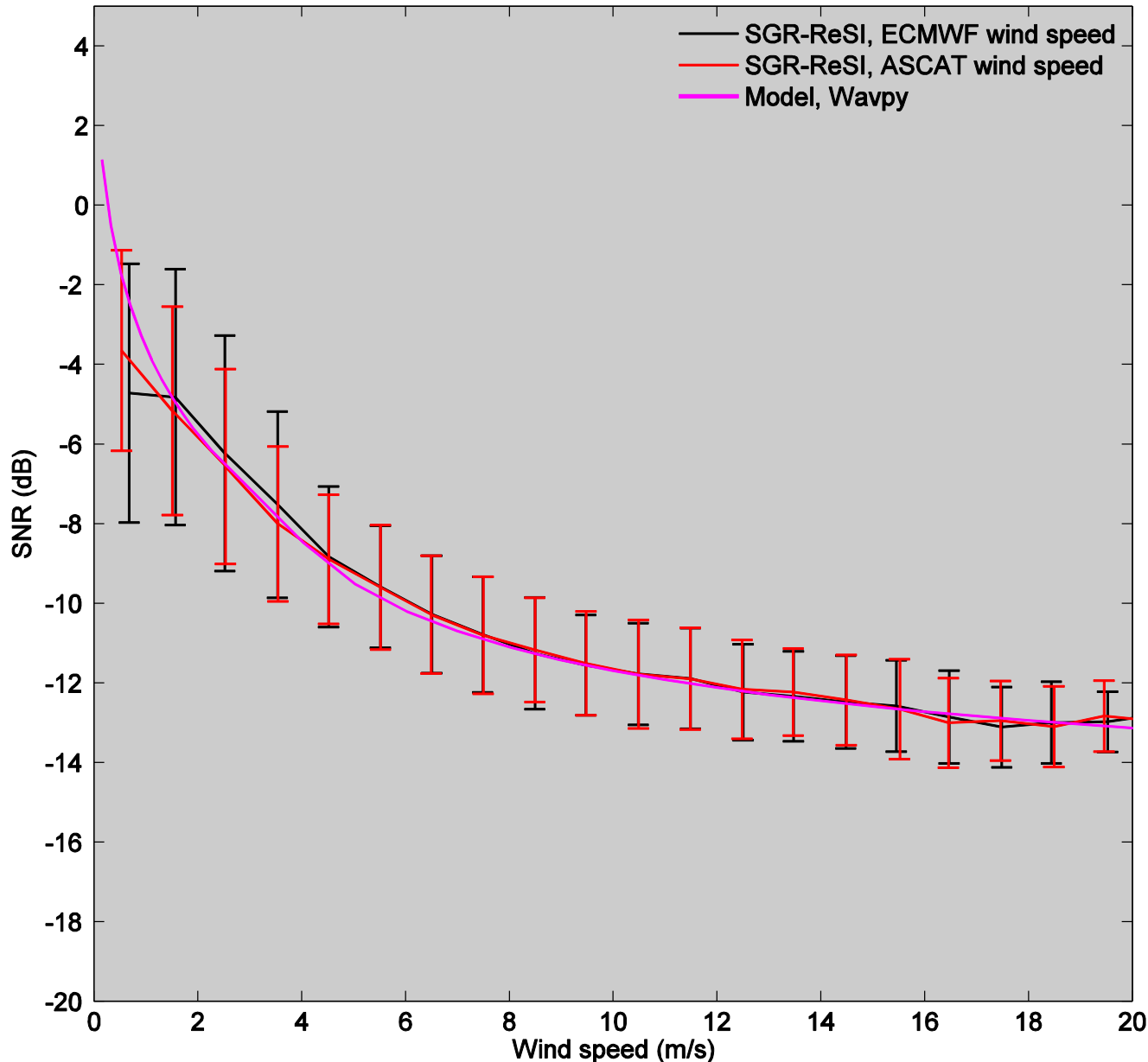


SNR₃ versus ASCAT wind speed



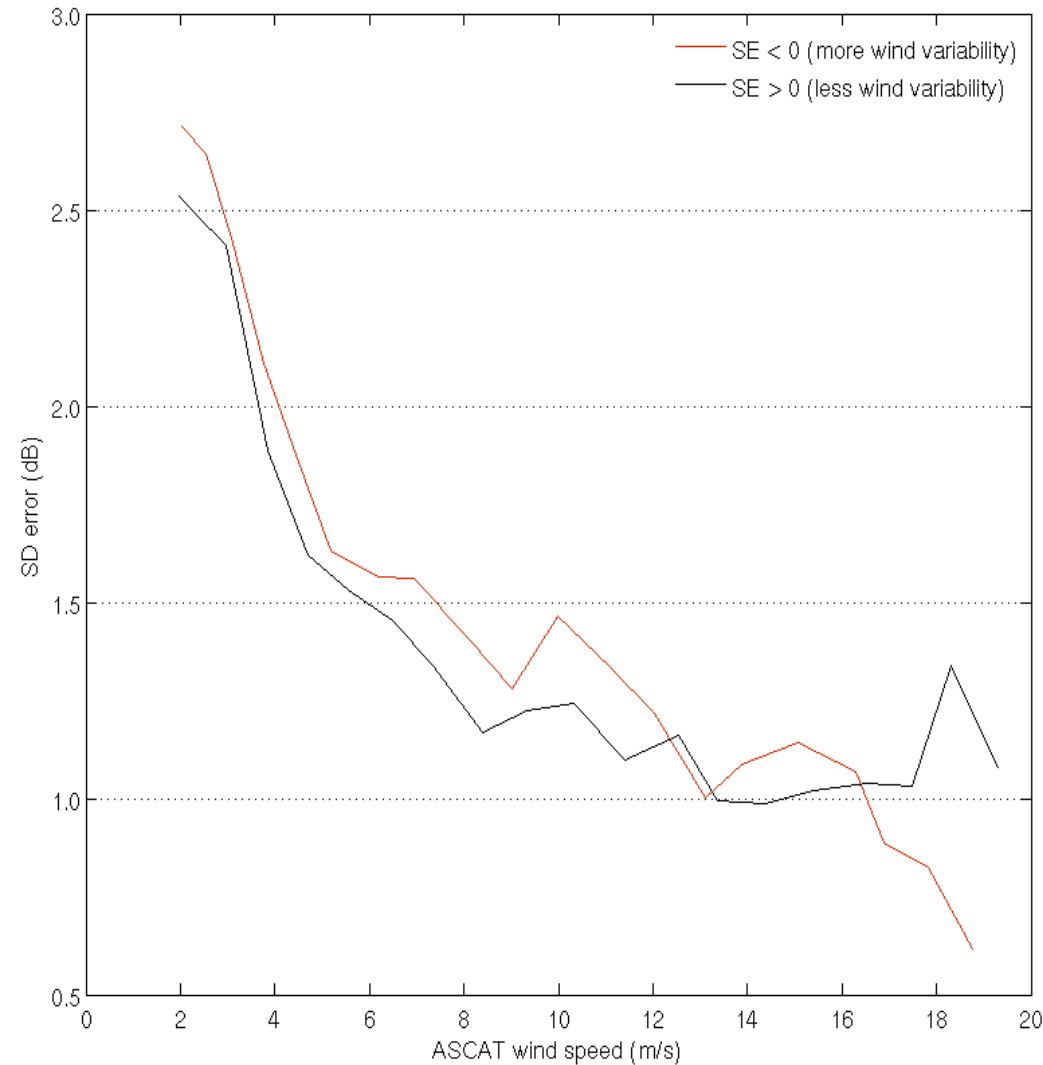
SNR₄ versus ASCAT wind speed

5. Analysis: observable vs ECMWF wind speed



SNR_4 fit has less uncertainty and better fits theoretical sensitivity (magenta curve) at low winds when using ASCAT winds (red curve) rather than ECMWF (black curve). This indicates that the SGR-ReSI actually measures the sea surface on a scale closer to that of ASCAT than that of ECMWF.

5. Analysis: observable vs ECMWF wind speed

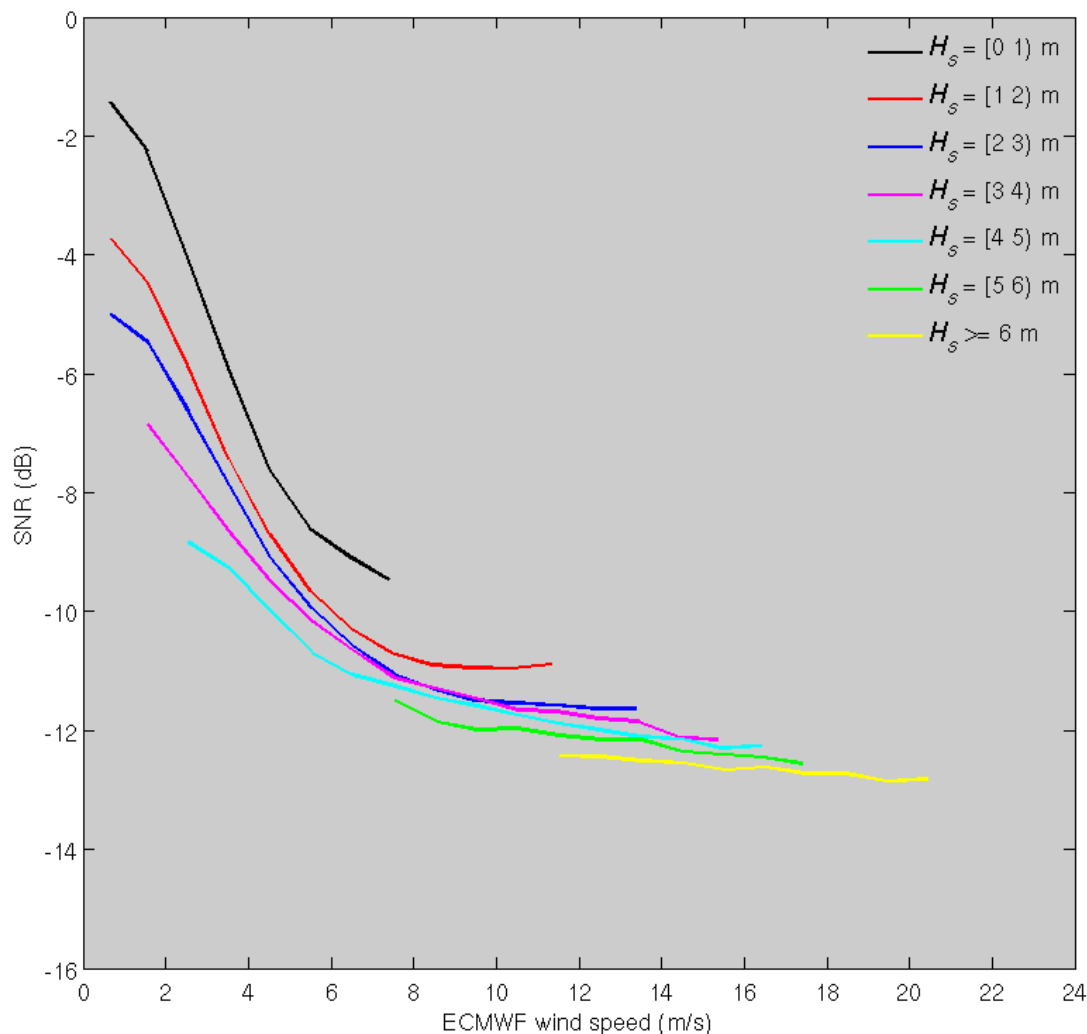


Negative SE (35%) values correspond to the less regular behaviour of ASCAT wind field (i.e., the high wind variability conditions)

Positive SE (65%) values indicate a more regular behaviour (i.e., the low wind variability conditions).

SD errors of SNR_4 as a function of ASCAT wind speed for different singularity exponent (SE) categories.

5. Analysis: observable vs wave parameters



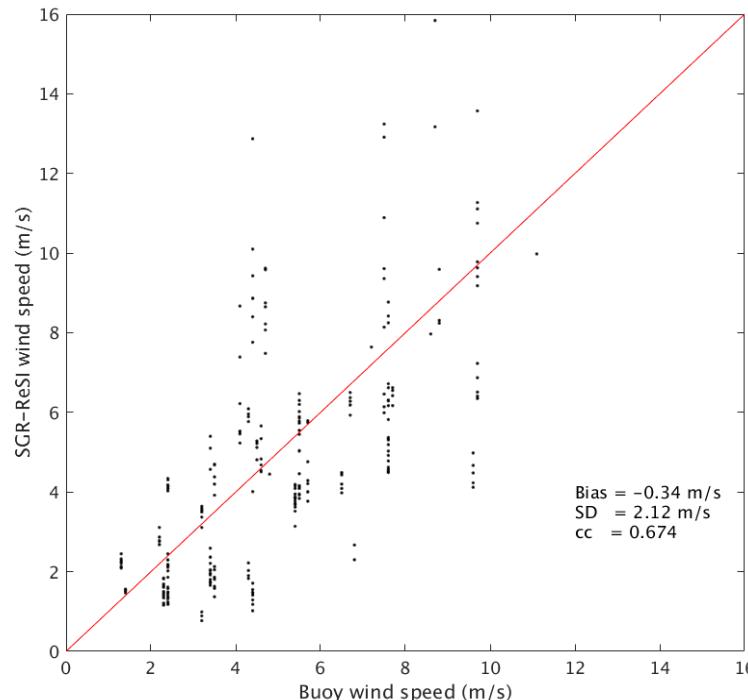
$H_s [0 \ 1)$: 3.9%
 $H_s [1 \ 2)$: 29.1%
 $H_s [2 \ 3)$: 34.5%
 $H_s [3 \ 4)$: 17.4%
 $H_s [4 \ 5)$: 8.6%
 $H_s [5 \ 6)$: 3.7%
 $H_s \geq 6$: 2.8%

Mean SNR_4 versus ECMWF wind speed
for different wave conditions (H_s , colors)

6. Wind validation: Triple collocation

SGR-ReSI winds (May-June 2015) provided by Giuseppe Foti (C-BRE data)

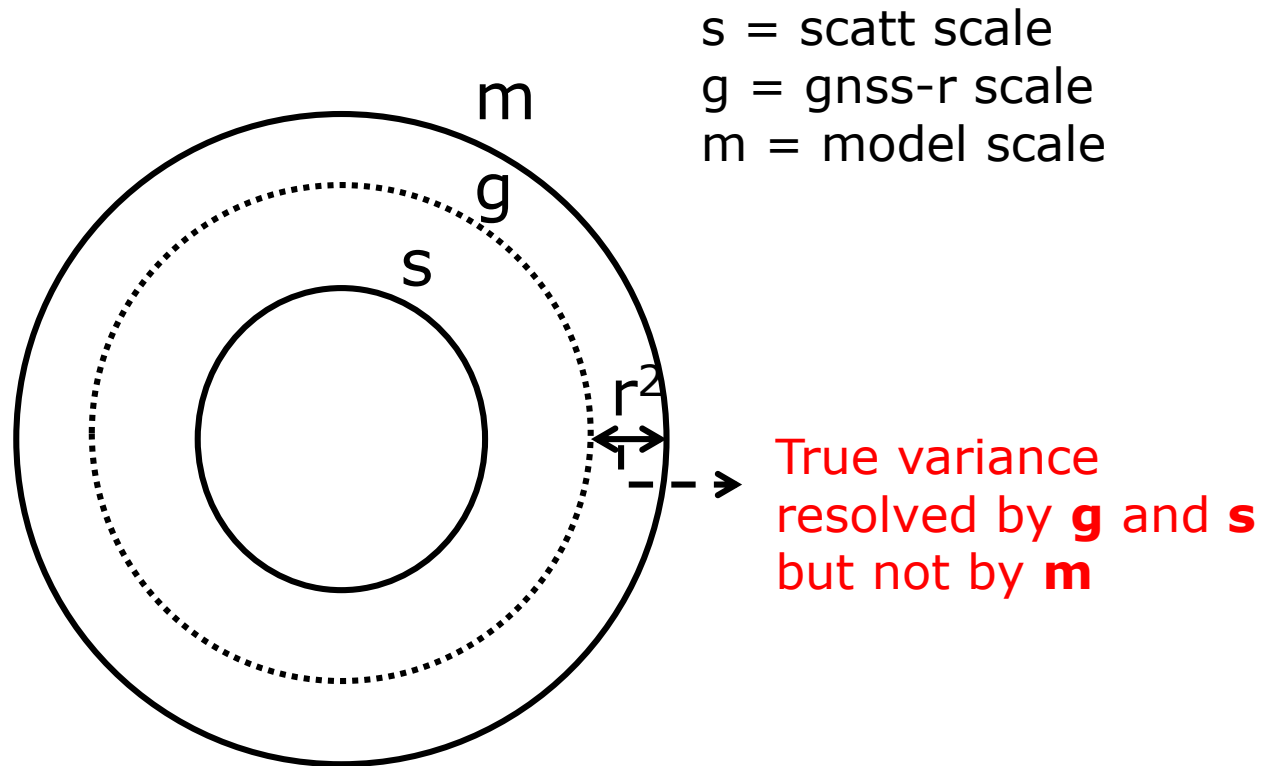
1. Collocated SGR-ReSI and buoy winds
2. Collocated SGR-ReSI, ASCAT and ECMWF winds
3. Collocated buoy, ASCAT and ECMWF winds (2009-
n of triple collocation analysis.



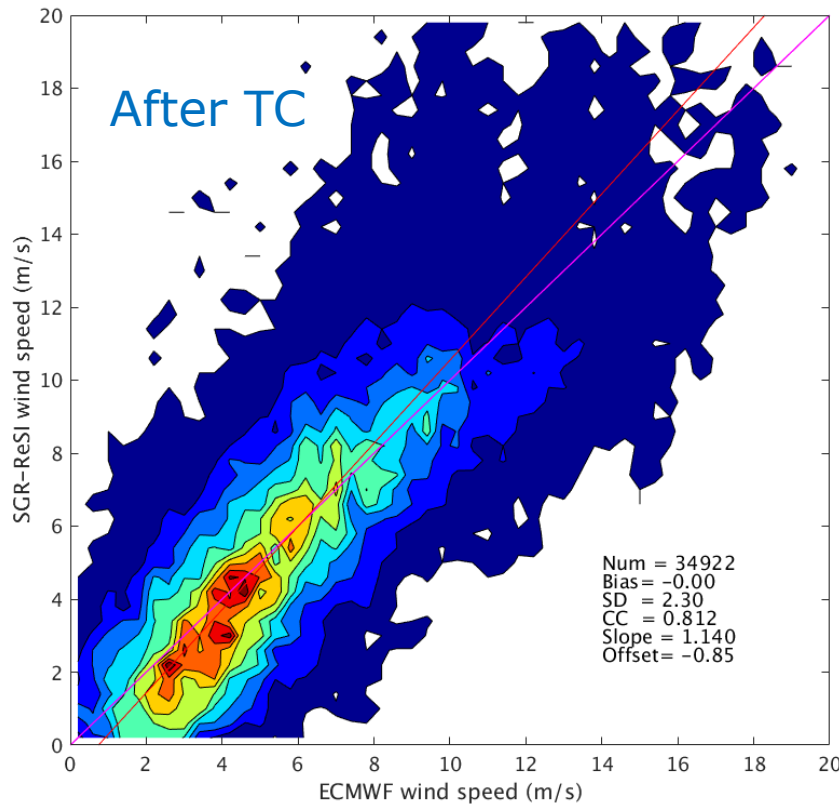
SGR-ReSI versus buoy winds (263 collocations)

- Bias = -0.34 m/s
- SD = 2.12 m/s
- CC = 0.674

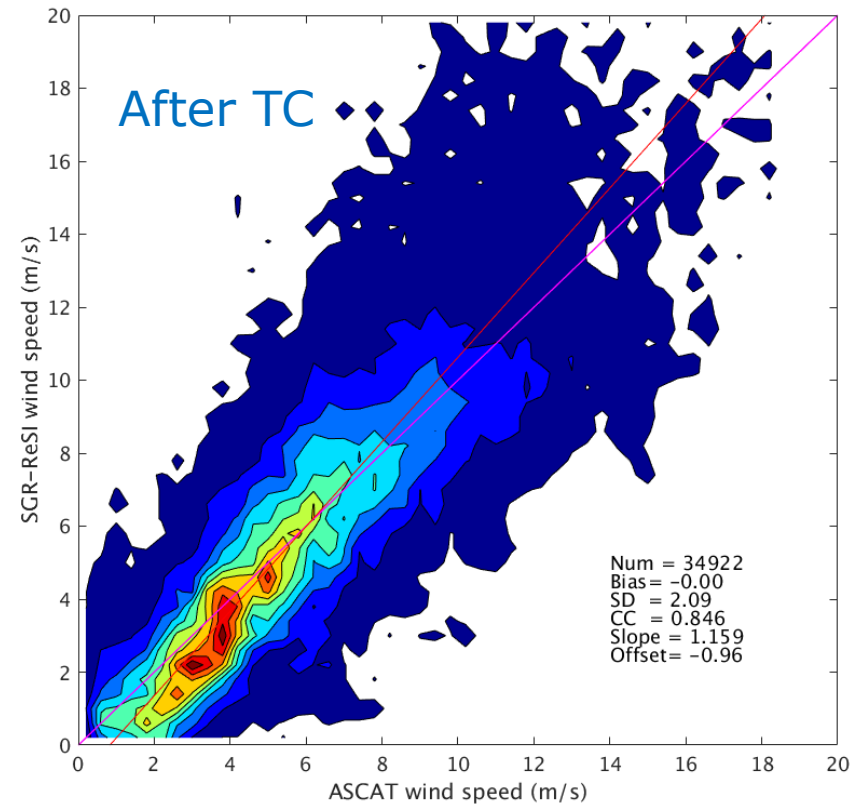
6. Wind validation: Triple collocation



6. Wind validation: Triple collocation



SGR-ReSI versus ECMWF winds



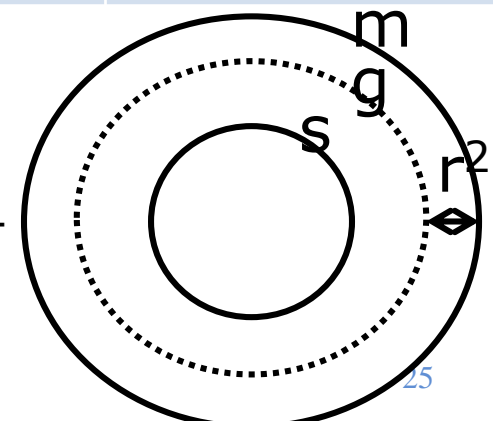
SGR-ReSI versus ASCAT winds

- The SGR-ReSI winds are closer to ASCAT winds than to ECMWF winds

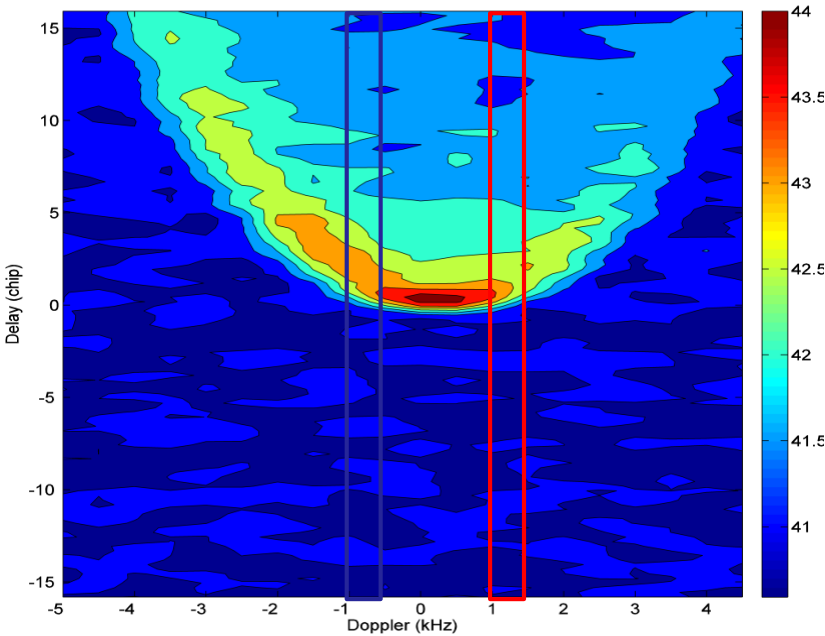
6. Wind validation: Triple collocation

In Sunlight	r^2 [m ² /s ²]	Scaling factor	Bias correction	ε [m/s] SGR-ReSI scales	ε [m/s] ECMWF scales
ASCAT	0.26	1.00	0.00	0.47 ± 0.003	0.70 ± 0.005
SGR-ReSI		1.22	0.66	2.04 ± 0.032	2.10 ± 0.034
ECMWF		1.05	-0.11	1.09 ± 0.015	0.94 ± 0.012
In Eclipse	r^2 [m ² /s ²]	Scaling factor	Bias correction	ε [m/s] SGR-ReSI scales	ε [m/s] ECMWF scales
ASCAT	0.09	1.00	0.00	0.47 ± 0.004	0.56 ± 0.005
SGR-ReSI		1.09	0.50	1.90 ± 0.043	1.93 ± 0.044
ECMWF		1.00	0.066	0.94 ± 0.018	0.89 ± 0.017

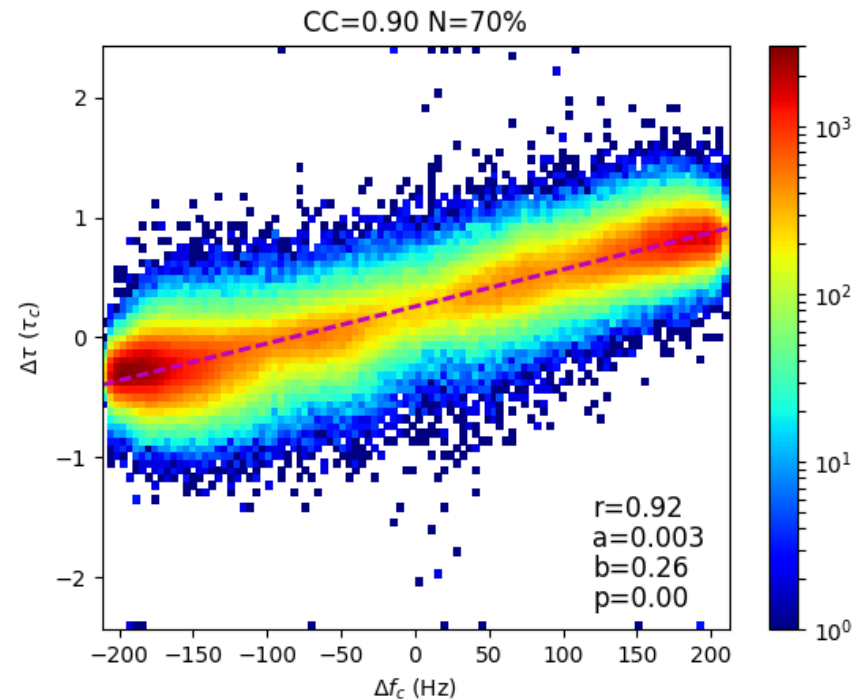
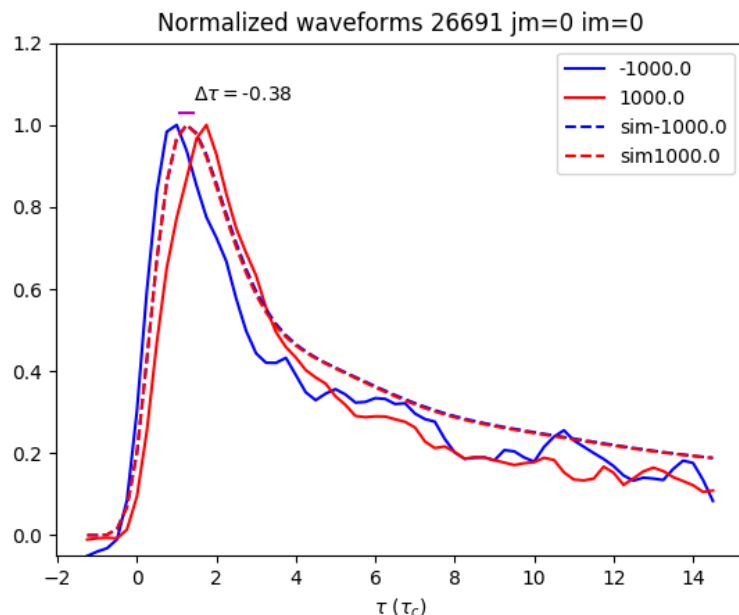
- SGR-ReSI wind speed SD errors around 2 m/s; larger in sunlight
- SGR-ReSI wind scales larger than those of ASCAT (due to noise)



DDM distortions (G. Grieco, KNMI)



- SP location error alters iso-delay / iso-Doppler symmetry
- This causes DDM asymmetry (see WFs @ ± 1 kHz shifted)
- Stare processing approach may be compromised



7. Conclusions

- Correction methods have been developed to substantially reduce the uncertainties in the measurements.
- ASCAT winds are more representative of SGR-ReSI SNRs than ECMWF winds, and therefore more suitable for deriving the SNR-to-wind GMF, particularly for low winds.
- DDMs in FGC mode are more sensitive to wind than those in UAGC mode. However, FGC SNRs have larger SD errors than UAGC SNRs, probably due to the larger discretization and/or satellite attitude error.
- Wind/Wave decoupling clearly visible in SGR-ReSI measurements, particularly for winds below 7 m/s.
- The overall SGR-ReSI SD errors are around 2 m/s; slightly larger in sunlight than in eclipse conditions, and certainly wind speed dependent.
- In addition, the estimated representativeness errors (r^2) show that although SGR-ReSI footprint is comparable to that of ASCAT, the retrieved winds are of significantly lower spatial resolution.